



## Polymer communication

## SAXS study on structure formation from the uniaxially oriented glass in isotactic polypropylene

S. Minami<sup>a</sup>, N. Tsurutani<sup>a</sup>, H. Miyaji<sup>a</sup>, K. Fukao<sup>b,1</sup>, Y. Miyamoto<sup>b,\*</sup><sup>a</sup>Department of Physics, Graduate School of Science, Kyoto University, Kyoto 606-8502 Japan<sup>b</sup>Department of Fundamental Sciences, Faculty of Integrated Human Studies, Kyoto 606-8501 Japan

Received 1 April 2003; received in revised form 17 October 2003; accepted 14 December 2003

**Abstract**

The structure formation of isotactic polypropylene from the uniaxially oriented glass into the smectic mesophase has been studied by small-angle X-ray scattering. Remarkable anisotropy between the directions parallel and perpendicular to the chain axis is found in the development of structure formation. Below  $-20\text{ }^{\circ}\text{C}$  is observed a structure with density variation having the wave vector,  $s$ , perpendicular to the chain axis with a period of 5 to 6 nm. Between  $-20$  and  $+25\text{ }^{\circ}\text{C}$ , the density variations with  $s$  both parallel and perpendicular to the chain axis develop. Above  $+25\text{ }^{\circ}\text{C}$ , the density variation with  $s$  perpendicular to the chain axis develops but disappears eventually, while that parallel to the chain axis keeps on growing.

© 2004 Elsevier Ltd. All rights reserved.

PACS: 61.43. - j; 61.41. + e; 61.20.Lc; 61.10.Eq

Keywords: Isotactic polypropylene; Smectic phase; Small-angle X-ray scattering

**1. Introduction**

The structure formation in the early stage of polymer crystallization has been a topic of growing interest. Prior to appreciable crystallization, the existence of the liquid crystal-like state and the change in the dynamics of molecular motion have been found in the ordering process from the glass [1,2]. Recently, a transient liquid crystalline mesophase has been also revealed in the crystallization process from the oriented amorphous state in poly(ethylene terephthalate) (PET) and copolymers [3–7].

It is well known that isotactic polypropylene (itPP) forms the “smectic” mesophase on quenching the melt into ice-water and on stretching in the solid state [8–10]. Through the smectic phase, crystallization from the glass takes place [11,12]. Crystallization from the sheared melt was also reported to occur through the smectic phase [13].

In a previous paper, we investigated the ordering process of itPP from the isotropic glass into the smectic phase by

small-angle X-ray scattering (SAXS) and wide-angle X-ray scattering (WAXS) [12]. We have observed the long period of 5–6 nm independent of temperature below about  $0\text{ }^{\circ}\text{C}$ , while it increases with temperature at higher temperatures. This result suggests that the different structure formation mechanisms operate below and above about  $0\text{ }^{\circ}\text{C}$ .

In this study, we examine and discuss the anisotropy of structure formation process from the itPP glass, and clarify the above difference in mechanism between the low and high temperatures; we have measured the temperature dependence and the time evolution of SAXS intensity during the transformation from the itPP glass drawn uniaxially into the oriented smectic phase.

**2. Experimental**

The material used is itPP ( $M_n = 1.2 \times 10^5$ ,  $M_w = 6.5 \times 10^5$ ) kindly supplied by Mitsubishi Chemical Corp. The itPP glass samples were prepared by melting the film samples 0.1 mm thick sandwiched by polyimide films 25  $\mu\text{m}$  thick at  $200\text{ }^{\circ}\text{C}$  for 10 min, followed by quenching into isopentane at  $-160\text{ }^{\circ}\text{C}$ . The glass samples were

\* Corresponding author.

E-mail address: [miyamoto@phys.h.kyoto-u.ac.jp](mailto:miyamoto@phys.h.kyoto-u.ac.jp) (Y. Miyamoto).<sup>1</sup> Department of Polymer Science, Kyoto Institute of Technology, Kyoto 606-8585 Japan.

stretched up to about four times the initial length in an ethanol bath at  $-40\text{ }^{\circ}\text{C}$ , lower than the lowest glass transition temperature ( $-30\text{ }^{\circ}\text{C}$ ) reported [12]. The drawn glass samples were kept below  $-50\text{ }^{\circ}\text{C}$  until they were placed in a heating cell for X-ray measurements; the cell was pre-cooled down to  $-50\text{ }^{\circ}\text{C}$ .

SAXS measurements were carried out at the High Intensity X-Ray Laboratory of Kyoto University. SAXS intensities were recorded using a two-dimensional position-sensitive proportional counter (2D PSPC) with the sample length being fixed. The peak intensity,  $I_{\text{peak}}$ , and the peak position,  $s_{\text{max}}$ , are determined by subtracting the scattering from foreign particles and the thermal diffuse scattering from the observed SAXS intensity. Hence  $I_{\text{peak}}$  is attributed to the electron density variation due to the structure formation. The detailed specifications of SAXS and WAXS systems, and the data correction method have been given elsewhere [12,14]. The exposure time for SAXS measurement was typically 30 min. The temperature and the annealing time given below are the average temperature and the average time during the data accumulation, respectively.

### 3. Results and discussion

Fig. 1a and b shows the SAXS intensity from the raw data obtained on heating the glass at 0.1 K/min in the equatorial and the meridional (drawing) directions, respectively, where  $s = 2 \sin \theta / \lambda$  is the magnitude of scattering vector, with the scattering angle  $2\theta$  and the X-ray wavelength  $\lambda$ . In the glassy state at  $-42\text{ }^{\circ}\text{C}$ , the intensity decreases monotonically

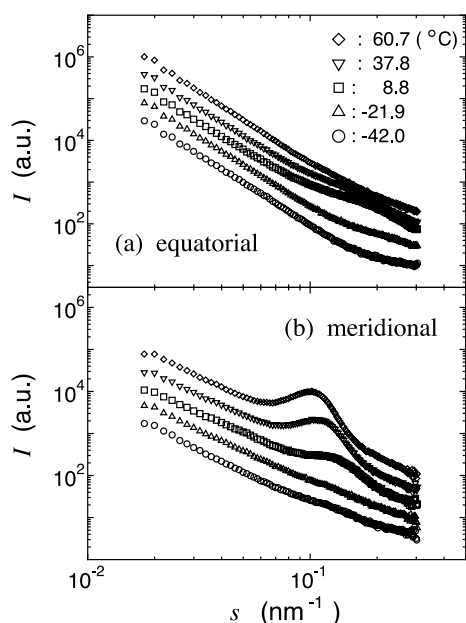


Fig. 1. SAXS intensity on heating at 0.1 K/min from the oriented glass at  $\circ$ :  $-42.0\text{ }^{\circ}\text{C}$ ,  $\triangle$ :  $-21.9\text{ }^{\circ}\text{C}$ ,  $\square$ :  $8.8\text{ }^{\circ}\text{C}$ ,  $\nabla$ :  $37.8\text{ }^{\circ}\text{C}$  and  $\diamond$ :  $60.7\text{ }^{\circ}\text{C}$ . (a) Equatorial and (b) meridional direction. The intensities are shifted vertically for comparison.

with scattering angle in both the equatorial and the meridional directions with a tail at high scattering angles due to the thermal density fluctuation. Since the intensity at low scattering angles remains almost unchanged on heating, it should be arising from the foreign particles [12,14]. Subtracting these contribution, we have no  $I_{\text{peak}}$  corresponding to the electron density variation concerned, and hence the as-drawn glass of itPP is uniform in electron density in the length scale of 3 to 50 nm corresponding to the range of scattering vector. At  $-22\text{ }^{\circ}\text{C}$ , the SAXS peak is observed only on the equator. In the meridional direction, the peak can be seen at  $+9\text{ }^{\circ}\text{C}$ . At  $60\text{ }^{\circ}\text{C}$ , the peak on the equator disappears.

The temperature dependences of  $I_{\text{peak}}$  in the equatorial and meridional directions are shown in Fig. 2a in the logarithmic scale, and that of the long period,  $L = 1/s_{\text{max}}$ , in Fig. 2b. In the equatorial direction, the SAXS peak becomes appreciable at about  $-30\text{ }^{\circ}\text{C}$ . However,  $I_{\text{peak}}$  and  $L$  cannot be determined quantitatively till  $-22\text{ }^{\circ}\text{C}$ , and hence we plot in Fig. 2 the data above  $-22\text{ }^{\circ}\text{C}$ . Up to  $+20\text{ }^{\circ}\text{C}$ ,  $I_{\text{peak}}$  and  $L$  increase with increasing temperature. Above  $+20\text{ }^{\circ}\text{C}$ , however,  $I_{\text{peak}}$  and  $L$  decrease with temperature, and disappears at about  $60\text{ }^{\circ}\text{C}$ . In the meridional direction, on the other hand, the temperature above which the SAXS peak becomes appreciable is about  $-15\text{ }^{\circ}\text{C}$ , higher than in the equatorial direction, and again we plot in Fig. 2 the data for  $I_{\text{peak}}$  and  $L$  above  $-7\text{ }^{\circ}\text{C}$ . Then  $I_{\text{peak}}$  increases with temperature more rapidly than in the equatorial direction, and  $L$  increases gradually with temperature. Around  $+20\text{ }^{\circ}\text{C}$ , both the equatorial and the meridional SAXS peaks ( $L$  is about 8 nm in both directions) are clearly observed as shown in Fig. 3.

WAXS patterns are taken from  $-40$  to  $20\text{ }^{\circ}\text{C}$  for itPP of a sample history similar to the SAXS heating measurement. The observed WAXS patterns are similar to those of the

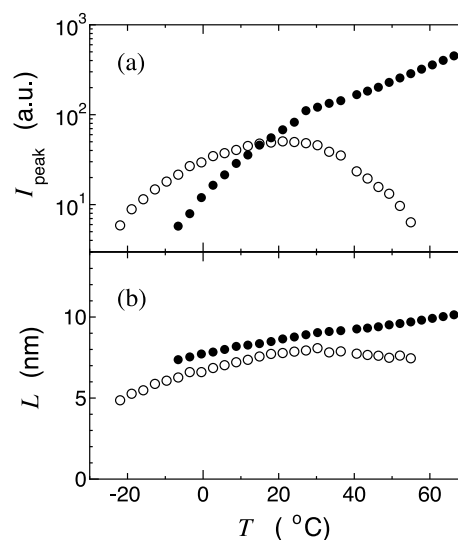


Fig. 2. Temperature dependence of (a) SAXS peak intensity and (b) long period on heating from the glass at 0.1 K/min. The equatorial direction ( $\circ$ ) and the meridional direction ( $\bullet$ ).

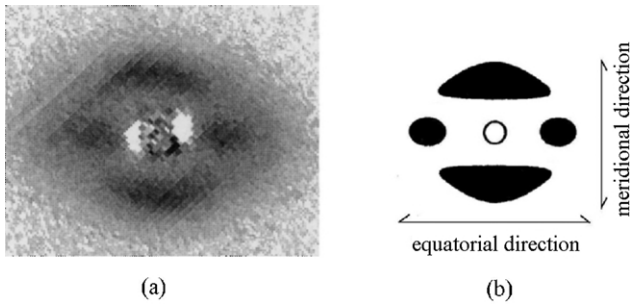


Fig. 3. (a) 2D PSC SAXS pattern at 24 °C and (b) schematic diagram. The stretching direction is vertical.

smectic phase formed by drawing below 70 °C [15–17]. However, the peak intensity increases slightly and the line width decreases with increasing temperature both on the equator and on the first layer line.

The time evolution of structure formation at a fixed temperature is investigated between  $-30$  and  $+45$  °C where no transformation into the monoclinic crystal phase occurs. The representative results for  $I_{\text{peak}}$  and  $L$  are shown in Figs. 4 and 5, respectively. Since the heating rate is as low as about 1 K/min from  $-50$  °C to the annealing temperature in order to prevent temperature overshooting, appreciable structure formation has already taken place before starting the SAXS measurements at a given temperature. The change in SAXS pattern with annealing time after heating up to a given temperature can be classified into the following three temperature regimes.

(1) Below  $-20$  °C,  $I_{\text{peak}}$  increases and  $L$  slightly increases with time in the equatorial direction, while no excess SAXS intensity is observed in the meridional direction (Figs. 4c and 5c).

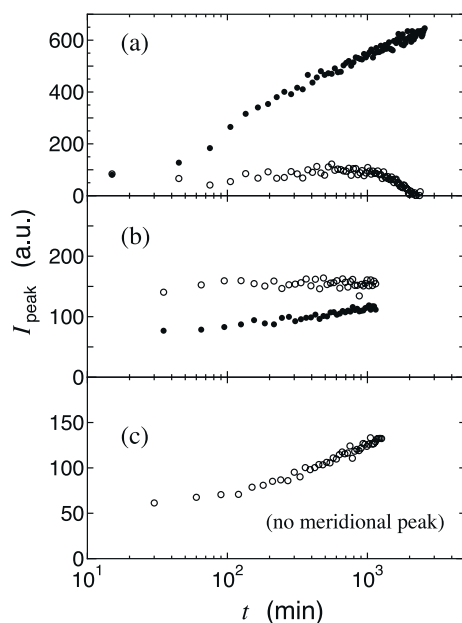


Fig. 4. Change in SAXS peak intensity on annealing at fixed temperatures at (a) 30.7 °C, (b)  $-2.6$  °C and (c)  $-28.6$  °C in the equatorial direction (○) and in the meridional direction (●).

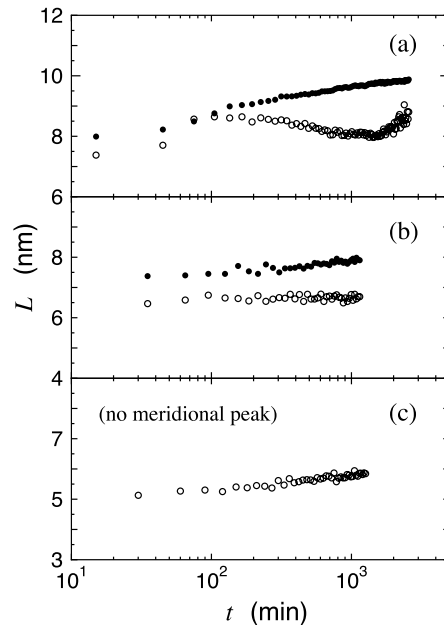


Fig. 5. Change in long period on annealing at fixed temperatures at (a) 30.7 °C, (b)  $-2.6$  °C and (c)  $-28.6$  °C in the equatorial direction (○) and in the meridional direction (●).

both the peaks on the equator and on the meridian develop. In the meridional direction,  $I_{\text{peak}}$  keeps increasing after that in the equatorial direction nearly stops increasing at about 100 min at  $-2.6$  °C in Fig. 4b. In these temperature and time ranges,  $L$  in the equatorial direction is almost independent of annealing time (Fig. 5b), however, it increases from 6 to 8 nm with annealing temperature. On the other hand,  $L$  in the meridional direction increases with time (Fig. 5b) and is larger at a higher temperature at a given annealing time. (3) Above  $+25$  °C,  $I_{\text{peak}}$  in the equatorial direction first increases and then decreases to disappear eventually (Fig. 4a). During the above change in intensity,  $L$  in the equatorial direction first increases, then decreases, and increases again before the SAXS peak disappears (Fig. 5a). The annealing time at which the intensity starts decreasing decreases with increasing annealing temperature. The change in  $I_{\text{peak}}$  in the meridional direction shows the approximate relation  $I_{\text{peak}} \propto \log t$ , and its slope increases with increasing temperature. The long period  $L$  also increases almost linearly with  $\log t$  and becomes larger with increasing temperature: at 100 min, 9 nm at 30.7 °C, and 10 nm at 44.0 °C.

The density variation in a length scale of several nm perpendicular to the chain axis is attributed to a fibrous structure with periodicity, and that parallel to the chain axis, to a stacked lamellar-like structure. To the best of the authors' knowledge, the appearance of the former fibrous structure has not been reported in neither the crystallization nor the pre-crystallization process so far. Fig. 2 shows that on heating the oriented glassy itPP the fibrous structure develops from about  $-22$  °C and disappears at about 60 °C. On the other hand, the lamellar structure is observed above

about  $-10\text{ }^{\circ}\text{C}$ , a temperature higher than the fibrous structure, and grows with increasing temperature. From these results, the different structure formation processes observed below and above  $0\text{ }^{\circ}\text{C}$  in the isotropic glass [12] can be attributed to that of the fibrous and the lamellar structures, respectively.

The crossover behavior in  $I_{\text{peak}}$  in the equatorial and meridional directions in Fig. 2a is interpreted in terms of the rate constant for the structure formation and the time scale of the present experiment:  $k_{\text{F}}$  is the rate of formation of the fibrous structure from the oriented amorphous phase,  $k_{\text{L}}$ , that of the lamellar structure from the oriented amorphous phase or from the fibrous structure, and  $\tau_{\text{obs}}$  is the timescale of observation, 10 to  $10^3$  min in the present experiment. Below  $-20\text{ }^{\circ}\text{C}$ ,  $k_{\text{F}} \sim 1/\tau_{\text{obs}} \gg k_{\text{L}}$ ; only the fibrous structure develops in this temperature range. Above  $-20\text{ }^{\circ}\text{C}$ ,  $k_{\text{F}} \sim k_{\text{L}} \sim 1/\tau_{\text{obs}}$ , and the formation rates increase with increasing temperature. Between  $-20$  and  $+25\text{ }^{\circ}\text{C}$ , the fibrous structure consumes almost whole amorphous itPP to be saturated and the lamellar structure develops. Above  $+25\text{ }^{\circ}\text{C}$ , the lamellar structure keeps developing at the expense of the fibrous structure.

The rates of structure formation are controlled by the segmental diffusion factor near the glass transition temperature,  $T_{\text{g}}$ , and the diffusion factor is controlled by the time characteristic of the primary  $\alpha$ -process. In a previous paper, it has been shown that  $T_{\text{g}}$  of the isotropic itPP increases from below  $-30\text{ }^{\circ}\text{C}$  up to about  $1\text{ }^{\circ}\text{C}$  by the formation of the smectic phase in the glass [12]. The present result suggests that this increase in  $T_{\text{g}}$  arises from the formation of fibrous structure. Hence,  $k_{\text{L}}$  is controlled by the characteristic time of the  $\alpha$ -process with  $T_{\text{g}} \approx 1\text{ }^{\circ}\text{C}$ , while  $k_{\text{F}}$ , by that with  $-30 \leq T_{\text{g}} \leq 1\text{ }^{\circ}\text{C}$  which increases with the development of the fibrous structure. The slowing down of kinetics with time,  $I_{\text{peak}} \propto \log t$ , may be accounted by the increase of  $T_{\text{g}}$  with the development of the smectic phase.

In summary, the structure formation process in itPP from the oriented glassy state into the smectic phase is investigated by the heating and the time-resolved SAXS measurements. Below  $-20\text{ }^{\circ}\text{C}$ , only the fibrous structure with a long period of about 5 nm is formed, and both the

fibrous and the lamellar structures are formed above  $-20\text{ }^{\circ}\text{C}$ . Above  $+25\text{ }^{\circ}\text{C}$ , both structures first develop with time but the fibrous structure finally disappears and the lamellar structure keeps growing.

## Acknowledgements

The authors wish to thank the committee of HIXLAB of Kyoto University for the use of SAXS system, and Dr M. Seki of Mitsubishi Chemical Corp. for supplying us the material. This work is partly supported by a Grant-in-Aid for Scientific Research from Japan Society for the Promotion of Science and from the Ministry of Education, Culture, Sports, Science and Technology of Japan.

## References

- [1] Imai M, Mori K, Mizutani T, Kaji K, Kanaya T. *Polymer* 1992; 33(4451):4457.
- [2] Fukao K, Miyamoto Y. *Phys Rev Lett* 1997;79:4613.
- [3] Welsh GE, Blundell DJ, Windle AH. *Macromolecules* 1998;31:7562.
- [4] Asano T, Baltá Calleja FJ, Flores A, Tanigaki M, Mina MF, Sawatari C, Itagaki H, Takahashi H, Hatta I. *Polymer* 1999;40:6475.
- [5] Blundell DJ, Mahendrasingam A, Martin C, Fuller W. *J Mater Sci* 2000;35:5057.
- [6] Mahendrasingam A, Martin C, Fuller W, Blundell DJ, Oldman RJ, MacKerron DH, Harvie JL, Riekel C. *Polymer* 2000;41:1217.
- [7] Fukao K, Koyama A, Tahara D, Kozono Y, Miyamoto Y, Tsurutani N. *J Macromol Sci Part B-Phys* 2003;B42:717.
- [8] Natta G, Corradini P. *Nuovo Cimento Suppl* 1960;15:40.
- [9] Miller RL. *Polymer* 1960;1:135.
- [10] Sobue H, Tabata Y. *J Polym Sci* 1959;39:427.
- [11] Hsu CC, Geil PH, Miyaji H, Asai K. *J Polym Sci, Pt B: Polym Phys* 1986;24:2379.
- [12] Miyamoto Y, Fukao K, Yoshida T, Tsurutani N, Miyaji H. *J Phys Soc Jpn* 2000;69:1735.
- [13] Li L, de Jeu WH. *Macromolecules* 2003;36:4862.
- [14] Miyamoto Y, Fukao K, Miyaji H. *Colloid Polym Sci* 1995;273:66.
- [15] de Candia F, Iannelli P, Staulo G, Vittoria V. *Colloid Polym Sci* 1988; 286:608.
- [16] Cohen Y, Saral RF. *Polymer* 2001;42:5865.
- [17] Ran S, Zong X, Fang D, Hsiao BS, Chu B, Phillips RA. *Macromolecules* 2001;34:2569.